

# Pion Dynamics at Finite Temperature

D. Toublan

Institut für theoretische Physik der Universität Bern  
CH-3012 Bern, Switzerland

## Abstract

The pion decay constant and mass are computed at low temperature within Chiral Perturbation Theory to two loops. The effects of the breaking of Lorentz Symmetry by the thermal equilibrium state are discussed. The validity of the Gell-Mann Oakes Renner relation at finite temperature is examined.

# 1 Introduction

The spontaneous breaking of chiral symmetry is believed to be a property of the strong interaction at zero temperature. If the temperature is finite different regimes appear. For sufficiently low temperatures chiral symmetry is still spontaneously broken, whereas for high temperatures it has to be restored according to asymptotic freedom. The way this restoration happens is not yet known and the transition temperature is estimated to be around 150 – 250 MeV (for a review of QCD at finite temperature see [1]).

The low temperature regime hadronic phase is dominated by the lightest particle occurring in the spectrum: the pion. The non-zero but small masses of the  $u$  and  $d$  quarks, which explicitly break chiral symmetry, make it a pseudo-Goldstone boson of the theory. Because of the lightness of these quarks, their masses can be treated as perturbations.

When the system is heated, the first particles to be produced are the pions, whereas the states that remain massive in the chiral limit ( $m_{\text{quarks}} \rightarrow 0$ ) are exponentially suppressed. The low-energy properties of the pions are essentially fixed by chiral symmetry. This leads to a wealth of low-energy theorems derived in current algebra at  $T = 0$ . For instance the Gell-Mann Oakes Renner (GOR) relation relates the pion decay constant and mass to the quark condensate and the quark mass (for simplicity all the quarks are put to the same mass  $\hat{m}$ ) [2]:

$$\frac{M_\pi^2 F_\pi^2}{\hat{m} \langle 0 | \bar{q}q | 0 \rangle} = -1 + O(\hat{m}). \quad (1.1)$$

A very efficient technique to analyze the corrections to these theorems is the use of effective Lagrangians. The low-energy effective theory of QCD is Chiral Perturbation Theory (ChPT) [3, 4, 5]. At zero temperature and non-zero quark masses, the GOR relation ceases to hold [4]. The goal of the present paper is to compute the temperature dependence of the quantities involved in the GOR relation and to see whether the latter still holds in the chiral limit.

The thermodynamics of a hadron gas and the quark condensate below the chiral phase transition have already been studied up to three loops in ChPT [6]. The question of the pion propagation at finite temperature has been addressed: the self-energy is known to two loops in ChPT [7], but the pion decay constant to one loop only [8].

The thermal equilibrium state is not Lorentz invariant. In ChPT this first explicitly shows up at the two-loop order. It is then important to compute up to this order to see what happens in the non-zero temperature case. For instance the appearance of two distinct pion decay constants – one for time and one for space –

begins at this order. This was already noted in [9] and is a known feature of some non-relativistic system such as the antiferromagnet [10].

A short presentation of ChPT at finite temperature in the Real Time Formalism is the subject of the next section. The two-point axial Green's function is computed in Section 3, the pion decay constants and mass in Section 4. The GOR relation at finite temperature is the subject of Section 5. It is derived from two Ward Identities relating the axial and pseudoscalar two-point Green's functions. Some of the consequences of these identities are also examined. The regularization and the chiral limit of T-dependent functions appearing in the corpus are appended.

## 2 Cool Chiral Perturbation Theory

A finite temperature effective theory rests on the zero temperature one. In the path integral formalism going from one to another is essentially a change of manifold over which one integrates: a torus replaces a plane [11]. The Real Time Formalism is used because we are investigating time-dependent Green's functions.

To make the presentation simpler, we will only give those results we consider necessary here. The reader is invited to consult [4, 5] for a more detailed discussion on ChPT at  $T = 0$ . We will restrict ourself to the case where all quarks have the same mass  $\hat{m}$ .

ChPT is an effective theory describing QCD at low energies. The  $N$ -flavour massless-quark QCD Lagrangian is symmetric under  $SU(N)_R \times SU(N)_L$ , the chiral group. It is assumed that a spontaneous chiral symmetry breakdown occurs,

$$SU(N)_R \times SU(N)_L \rightarrow SU(N)_V,$$

whose Goldstone bosons are identified as the pions.

The QCD Lagrangian can be approximated at a given order in the momentum using an effective Lagrangian expressed in terms of a field  $U \in SU(N)$  which transforms linearly under  $SU(N)_R \times SU(N)_L$ ,

$$U \rightarrow g_R U g_L^+,$$

and contains the fields of the pseudoscalar Goldstone bosons,

$$U = e^{i\pi^a \tau_a / F}, \tag{2.1}$$

where  $\tau^a$  are the generators of  $SU(N)$  and  $F$  is the pion decay constant in the chiral limit:  $F_\pi = F(1 + O(\hat{m}))$ .

Coupling  $U$  with external fields and expanding the effective Lagrangian in powers of the external momenta and of quark masses, gives

$$\mathcal{L}_{\text{eff}} = \mathcal{L}^{(2)} + \mathcal{L}^{(4)} + \mathcal{L}^{(6)} + \dots \quad (2.2)$$

The promotion of the global chiral symmetry to a local one requires the introduction of a derivative  $\nabla_\mu U$  which is covariant with respect to the external axial and pseudoscalar gauge fields.

To get the desired  $O(p^6)$  accuracy, the tree, one- and two-loop diagrams of  $\mathcal{L}^{(2)}$ , the tree and one-loop graphs of  $\mathcal{L}^{(4)}$  and the trees of  $\mathcal{L}^{(6)}$  are needed.

We will restrict ourselves to the two flavour case ( $N = 2$ ) and use the traditional notation of [5]:  $\chi = 2B\hat{m} \mathbf{I} + 2iBp$ ,  $\nabla_\mu = \partial_\mu U - i\{a_\mu, U\}$  and  $F_{R,L}^{\mu\nu} = \pm\partial^\mu a^\nu \mp \partial^\nu a^\mu - i[a^\mu, a^\nu]$ , where  $B$  is proportional to the quark condensate in the massless quark limit. It is found that the parts of the Lagrangian that contribute to the axial and pseudoscalar two-point Green's functions to  $O(p^6)$  are:

1) Lowest order:

$$\mathcal{L}^{(2)} = \frac{F^2}{4} \langle \nabla_\mu U^\dagger \nabla^\mu U + \chi U^\dagger + \chi^\dagger U \rangle \quad (2.3)$$

2) Second order:

$$\begin{aligned} \mathcal{L}^{(4)} = & L_1 \langle \nabla_\mu U^\dagger \nabla^\mu U \rangle^2 + L_2 \langle \nabla_\mu U^\dagger \nabla_\nu U \rangle \langle \nabla^\mu U^\dagger \nabla^\nu U \rangle \\ & + L_4 \langle \chi U^\dagger + \chi^\dagger U \rangle \langle \nabla_\mu U^\dagger \nabla^\mu U \rangle + L_6 \langle \chi U^\dagger + \chi^\dagger U \rangle^2 \\ & + L_8 \langle \chi U^\dagger \chi U^\dagger + \chi^\dagger U \chi^\dagger U \rangle + L_{10} \langle U^\dagger F_R^{\mu\nu} U F_{L\mu\nu} \rangle \\ & + H_1 \langle F_R^{\mu\nu} F_{R\mu\nu} + F_L^{\mu\nu} F_{L\mu\nu} \rangle + H_2 \langle \chi^\dagger \chi \rangle \end{aligned} \quad (2.4)$$

3) Third order: the singular part of the two-point function we are interested in only receive  $T$ -independent corrections from the trees of  $\mathcal{L}_{\text{eff}}$  (see Section 3 for an illustration of this property at one loop). Hence  $\mathcal{L}^{(6)}$  won't be explicitly needed here.

When the temperature  $\beta^{-1}$  is non-zero, the fields  $U(x)$  map the  $\beta$ -dependent torus into  $SU(N)$ . The generating functional of the connected Green's functions is:

$$\exp \{ iZ[a_\mu, p] \} = \int [dU] \exp \left\{ i \int_C d^3x d\tau \mathcal{L}_{\text{eff}} \right\}. \quad (2.5)$$

The integration extends over  $\mathbb{R}^3$  and a contour  $C$ . In the Real Time Formalism of quantum field theory at finite temperature, which has been thoroughly studied in [11], one can choose different integration paths in the complex  $t$ -plane. We take the so-called Keldysh path shown in Figure 1. The functional integral extends

over field configurations with the boundary condition  $U(-\infty, \vec{x}) = U(-\infty - i\beta, \vec{x})$ , which is the familiar periodicity condition. A generalization of time-ordering has to be introduced:  $T$  is replaced by  $T_C$ , an operator which orders operators according to the occurrence of their time-arguments on the contour. A Heaviside,  $\theta_C$ , and a Dirac,  $\delta_C$ , distributions are defined on the contour [11].

The thermal propagator is a Green's function on the contour:

$$(\square_C + M^2) D_\beta(x - y) = \delta_C(x - y). \quad (2.6)$$

The unique solution satisfying the Kubo-Martin-Schwinger boundary condition is

$$\begin{aligned} D_\beta(\tau - \tau'; \omega_k) &= -\frac{i}{2\omega_k} e^{\beta\omega_k} n_B(\omega_k) \\ &\quad \left\{ \left[ e^{-i\omega_k(\tau - \tau')} + e^{-\beta\omega_k + i\omega_k(\tau - \tau')} \right] \theta_C(\tau - \tau') \right. \\ &\quad \left. + \left[ e^{i\omega_k(\tau - \tau')} + e^{-\beta\omega_k - i\omega_k(\tau - \tau')} \right] \theta_C(\tau' - \tau) \right\}, \end{aligned} \quad (2.7)$$

where  $n_B(x) = 1/(e^{\beta x} - 1)$  is the Bose distribution and  $\omega_k = \sqrt{\vec{k}^2 + M^2}$ .

When (2.5) is used to compute Green's functions with arguments on the real  $t$ -axis, only a part of  $Z[a_\mu, p]$  is relevant: the  $C_1$  and  $C_2$  contour segments are the important ones.

The introduction of the usual  $2 \times 2$  formalism allows us to rewrite the generating functional as ( $j = a_\mu, p$ ):

$$Z[j_1, j_2] = \int [dU_1][dU_2] \exp \left\{ i \int \frac{1}{2} U_m D_\beta^{-1 mn} U_n - V[U_1] + V[U_2] + j_n U_n \right\}, \quad (2.8)$$

where  $m, n = 1, 2$ , and  $j_1(x) = j(x)$ ,  $j_2(x)$  are independent sources.

The real-time Green's functions are generated by differentiating (2.8) with respect to  $j_1$  and setting both  $j_1$  and  $j_2$  to zero. For instance the real time two-point axial Green's function is given by:

$$\begin{aligned} i\langle T A_\mu^a(x) A_\nu^b(y) \rangle_T &= \frac{1}{\text{Tr} e^{-\beta H}} \text{Tr} \left\{ e^{-\beta H} T A_\mu^a(x) A_\nu^b(y) \right\} \\ &= \frac{\delta^2}{\delta a_{1\mu}^a(x) \delta a_{1\nu}^b(y)} Z[a_{1\mu}, a_{2\mu}, p_1, p_2] \Big|_{a_{1\mu} = a_{2\mu} = p_1 = p_2 = 0}. \end{aligned} \quad (2.9)$$

In momentum space the propagator  $D_\beta^{mn}$  reads:

$$\begin{cases} iD_\beta^{11}(k) = [iD_\beta^{22}(k)]^* = \tilde{\Delta}(k) + 2\pi \delta(k^2 - M^2) n_B(|k_0|) =: \tilde{\Delta}_\beta(k) \\ iD_\beta^{12}(k) = iD_\beta^{21}(k) e^{-\beta|k_0|} = 2\pi \delta(k^2 - M^2) n_B(|k_0|) \end{cases}, \quad (2.10)$$

where  $\tilde{\Delta}(k) = i/(k^2 - M^2 + i\varepsilon)$  is the usual Feynman propagator.

The topological and combinatorial structures of the Feynman diagrams do not change, but the propagator has now acquired a matrix structure and there are two kinds of fields. In a real-time Green's function only the type 1 field can appear on an external leg and the type 2 field plays the role of a ghost field. There are also two kinds of vertices, which are equivalent up to a sign. The two different fields interact through the off-diagonal terms of the propagator.

### 3 The axial two-point Green's function

The finite temperature two-point Green's function of the axial current

$$A_\mu^a(x) = \bar{q}(x) \frac{\tau^a}{2} \gamma_\mu \gamma_5 q(x) \quad (3.1)$$

describes the dynamics of a pion in a strongly interacting gas ( $\tau^a$  are the  $SU(2)$  generators). Let  $G_{\mu\nu}(x-y, T) \delta^{ab} := i \langle T A_\mu^a(y) A_\nu^b(y) \rangle_T$ . In general the two-point axial Green's function at finite temperature can be written as:

$$\tilde{G}_{\mu\nu}(q, T) = - \frac{q_\mu q_\nu \alpha^A(q, T) + q_\mu \beta_\nu^A(q, T) + q_\nu \beta_\mu^A(q, T) + \gamma_{\mu\nu}^A(q, T)}{q_0^2 - \Xi(q, T)} + \rho_{\mu\nu}^A(q, T) \quad (3.2)$$

It contains a singular piece and a finite part,  $\rho_{\mu\nu}^A(q, T)$ . To get this Green's function to order  $T^4$  in  $SU(2)$ -ChPT (two flavours), one needs to compute the Feynman graphs shown in Figure 2 with the effective Lagrangian (2.2).

The singular parts of the tree diagrams are temperature independent. They just contain the zero temperature Feynman propagator  $\tilde{\Delta}(q)$ . Most of them have already been computed in [4, 12]. The other components of the matrix propagator generate imaginary parts of the finite term of the two-point Green's function. Thus they are not interesting in our context. They will only be mentioned in the one-loop computation given below and ignored elsewhere.

The  $T$ -dependence of the one-loop graphs is rather simple: only properties of the thermal propagator at the origin appear in that case [4].

At lowest order the pion mass is

$$M^2 := 2\hat{m}B \quad (3.3)$$

and the various  $O(p^4)$  graphs are:

$$\tilde{G}_{\mu\nu}^{(4.1+4)}(q, T) = g_{\mu\nu} \left( F^2 + 16M^2 L_4 - 2\Delta_\beta(0) \right) \quad (3.4)$$

$$\begin{aligned}
& +[q^2 g_{\mu\nu} - q_\mu q_\nu] (4H_1 - 2L_{10}) \\
\tilde{G}_{\mu\nu}^{(4.2+5)}(q, T) &= q_\mu q_\nu \left( \frac{8}{3} \Delta_\beta(0) + 32L_4 M^2 \right) \tilde{\Delta}_\beta(q) \tag{3.5}
\end{aligned}$$

$$\begin{aligned}
\tilde{G}_{\mu\nu}^{(4.3+6)}(q, T) &= i q_\mu q_\nu \left( \frac{4q^2 - M^2}{6} \Delta_\beta(0) \right. \\
& \left. + M^2(-16L_4 q^2 + 32L_6 M^2 + 16L_8 M^2) \right) \left[ (\tilde{\Delta}_\beta(q))^2 - (iD_\beta^{12}(q))^2 \right]. \tag{3.6}
\end{aligned}$$

The relation  $(\square + M^2)\Delta_\beta(x) = i\delta^{(d)}(x)$  has been used to simplify the expressions.

At first sight, the term in square brackets in (3.6) seems to be ill defined: it contains products of Dirac distributions with the same argument. But the equation of motion implies that

$$\begin{aligned}
\partial_{M^2} \Delta_\beta(x) &= i \frac{d}{dM^2} D_\beta^{11}(x) \tag{3.7} \\
&= -i \int d^d y \left( D_\beta^{11}(x-y) D_\beta^{11}(y) - D_\beta^{12}(x-y) D_\beta^{12}(y) \right).
\end{aligned}$$

Hence the products of thermal statistical weights at intermediate stages of the computation disappear when the different types of vertices are combined. This is a generic feature of the Real Time Formalism [11].

Moreover the terms coming from the thermal parts of  $\Delta_\beta(q)$  and the alike only contribute to  $\rho_{\mu\nu}^A(q, T)$ , the finite term of the two-point function. To get the pole and residue of the latter, it suffice to replace  $\Delta_\beta(q)$  by the corresponding Feynman propagator everywhere. This is the case to all orders in the perturbation.

The functions appearing in (3.2) at first non-leading order are already known [8]:

$$\begin{aligned}
\Xi(q, T) &= \vec{q}^2 + M^2 \left\{ 1 + \frac{M^2}{F^2} [-16L_4 + 32L_6 + 16L_8] \right\} \\
& \quad + \frac{M^2}{2F^2} \Delta_\beta(0) + O(p^6), \tag{3.8}
\end{aligned}$$

$$\alpha^A(q, T) = F^2 \left\{ 1 + \frac{M^2}{F^2} [16L_4] \right\} - 2\Delta_\beta(0) + O(p^6), \tag{3.9}$$

$$\begin{aligned}
\beta_\mu^A &= O(p^6), & \gamma_{\mu\nu}^A &= O(p^6), \\
\rho_{\mu\nu}^A(q, T) &= g_{\mu\nu} \left( F^2 + 16M^2 L_4 - 2\Delta_\beta(0) \right) \\
& \quad + [q^2 g_{\mu\nu} - q_\mu q_\nu] (4H_1 - 2L_{10}) + O(p^6). \tag{3.10}
\end{aligned}$$

Only  $\rho_{\mu\nu}^A(q, T)$  really depends on the momentum. As already said, the Lorentz symmetry is not explicitly broken at this order.

Because  $\Delta_\beta(0)$  contains the Feynman propagator at the origin, it diverges. As usual in ChPT, because it preserves the symmetry of the theory, dimensional regularization is used [4, 6]:

$$\Delta_\beta(0) = \int \frac{d^d k}{(2\pi)^d} \tilde{\Delta}_\beta(k) = 2M^2\lambda + \mathcal{N}_M(T), \quad (3.11)$$

where

$$\lambda = \frac{\mu^{d-4}}{(4\pi)^2} \left( \frac{1}{d-4} - \frac{1}{2} [\ln 4\pi + \Gamma'(1) + 1] + \ln\left(\frac{M}{\mu}\right) + O(d-4) \right), \quad (3.12)$$

and

$$\mathcal{N}_M(T) = \int \frac{d^4 k}{(2\pi)^3} \delta(k^2 - M^2) n_B(\omega_k). \quad (3.13)$$

The renormalization of the theory at finite temperature has to be the same as at  $T = 0$ . This is obviously here the case: no divergence occur in the temperature dependent part of the two-point function. The scale independent parameters used to renormalize the theory are:

$$\bar{L}_i = L_i - \gamma_i \lambda, \quad \bar{H}_i = H_i - \delta_i \lambda, \quad (3.14)$$

where  $\gamma_1 = 1/12$ ,  $\gamma_2 = 1/6$ ,  $\gamma_4 = 1/4$ ,  $\gamma_6 = 3/32$ ,  $\gamma_8 = 0$ ,  $\gamma_{10} = 2/3$ ,  $\delta_1 = 1/3$  and  $\delta_2 = 0$ . In ChPT at  $T = 0$ , the expansion of the pion mass and decay constant at  $O(p^4)$  can be expressed in terms of  $F$ ,  $M$  and  $\bar{L}_i$ :

$$M_\pi^2 = M^2 \left\{ 1 + \frac{M^2}{F^2} [-16\bar{L}_4 + 32\bar{L}_6 + 16\bar{L}_8] \right\} + O(p^6), \quad (3.15)$$

$$F_\pi^2 = F^2 \left\{ 1 + \frac{M^2}{F^2} [16\bar{L}_4] \right\} + O(p^6) \quad (3.16)$$

The  $O(p^6)$  graphs are a bit more complicated than those of  $O(p^4)$ . However, only the  $T$ -dependent terms are of interest here. Thus the diagrams (6.23 – 28) will not be explicitly given (see [12, 13, 14] for an analysis of zero temperature ChPT to  $O(p^6)$ ).

Some of the two-loop graphs, (6.1 – 3, 6.13 – 16), are just products of lower order ones.

The diagrams (6.4 – 6, 6.17 – 19) involve essentially the same elements as those occurring at one loop. Only their vertices are different: they contain some low-energy coupling constants and derivatives. For instance the graphs (6.5) and (6.18) give:

$$\tilde{G}_{\mu\nu}^{(6.5)} = -\frac{8i}{3F^2} q_\mu q_\nu \tilde{\Delta}(q) \Delta_\beta^2(0), \quad (3.17)$$



$$\begin{aligned} \tilde{G}_{\mu\nu}^{(6.18)} &= \frac{16i}{F^2} \tilde{\Delta}(q) \int \frac{d^d k}{(2\pi)^d} \tilde{\Delta}_\beta(q) \left\{ (2L_1 + 4L_2) k q (k_\nu q_\mu + k_\mu q_\nu) \right. \\ &\quad \left. + (6k^2 L_1 + 2k^2 L_2 - \frac{17}{3} M^2 L_4) q_\mu q_\nu \right\}. \end{aligned} \quad (3.18)$$

The graphs (6.7 – 9, 6.20 – 22) are special ones for the Real Time Formalism. They are the only diagrams in the whole set which contribute to the pole and residue of the two-point function and contain type 2 fields. Their role is very important for the consistency of the theory [11]. The graphs (6.8) and (6.21) are taken as examples:

$$\begin{aligned} \tilde{G}_{\mu\nu}^{(6.8)} &= -\frac{4}{9F^2} q_\mu q_\nu \tilde{\Delta}(q) \Delta_\beta(0) \\ &\quad \int \frac{d^d k}{(2\pi)^d} (4k^2 - M^2) \left[ (iD_\beta^{11}(k))^2 - (iD_\beta^{12}(k))^2 \right], \end{aligned} \quad (3.19)$$

where the fact that the type-2 tadpole is the same as the type-1 tadpole has been used, and

$$\begin{aligned} \tilde{G}_{\mu\nu}^{(6.21)} &= \frac{128M^2}{3F^2} q_\mu q_\nu \tilde{\Delta}(q) \int \frac{d^d k}{(2\pi)^d} (k^2 L_4 - 2M^2 L_6 - M^2 L_8) \\ &\quad \left[ (iD_\beta^{11}(k))^2 - (iD_\beta^{12}(k))^2 \right]. \end{aligned} \quad (3.20)$$

As a consequence of (3.7), the integrals in (3.19,3.20) are essentially  $\partial_{M^2} \Delta_\beta(0)$ . In  $d = 4$ , this quantity contains a singular piece:

$$\partial_{M^2} \Delta_\beta(0) = 2\lambda + \frac{1}{16\pi^2} + \partial_{M^2} \mathcal{N}_M(T). \quad (3.21)$$

Finally, we turn to the genuine two-loop graphs. These are the closed-eye (6.10), the gumbard (6.11) and the sunset (6.12), given by:

$$\begin{aligned} \tilde{G}_{\mu\nu}^{(6.10)}(q, T) &= -\frac{4}{9F^2} \int \frac{d^d k_1 d^d k_2}{(2\pi)^{2d}} \tilde{\Delta}_\beta(k_1) \tilde{\Delta}_\beta(k_2) \tilde{\Delta}_\beta(q - k_1 - k_2) \\ &\quad \left\{ (3k_{1\mu} + 3k_{2\mu} - 2q_\mu) (3k_{1\nu} + 3k_{2\nu} - 2q_\nu) \right\}, \end{aligned} \quad (3.22)$$

$$\begin{aligned} \tilde{G}_{\mu\nu}^{(6.11)}(q, T) &= \frac{2}{9F^2} q_\mu \tilde{\Delta}(q) \int \frac{d^d k_1 d^d k_2}{(2\pi)^{2d}} \tilde{\Delta}_\beta(k_1) \tilde{\Delta}_\beta(k_2) \tilde{\Delta}_\beta(q - k_1 - k_2) \\ &\quad (2q_\nu - 3k_{1\nu} - 3k_{2\nu}) \left\{ k_1^2 + k_2^2 + 4k_1 k_2 + M^2 + 2(k_1 + k_2)q - 2q^2 \right\} \\ &\quad + (\mu \longleftrightarrow \nu), \end{aligned} \quad (3.23)$$

$$\begin{aligned} \tilde{G}_{\mu\nu}^{(6.12)}(q, T) &= -\frac{i}{18F^2} q_\mu q_\nu \tilde{\Delta}^2(q) \int \frac{d^d k_1 d^d k_2}{(2\pi)^{2d}} \tilde{\Delta}_\beta(k_1) \tilde{\Delta}_\beta(k_2) \tilde{\Delta}_\beta(q - k_1 - k_2) \\ &\quad \left\{ 3M^4 + (k_1^2 + k_2^2 + 4k_1 k_2 + M^2 + 2(k_1 + k_2)q - 2q^2)^2 \right\}. \end{aligned} \quad (3.24)$$

One readily sees that the polynomials appearing in the integrands are essentially four-point functions at tree level. For instance the square of the tree-level isospin averaged  $\pi$ - $\pi$  scattering amplitude appears in the sunset. These integrals may first appear complicated, but using the symmetry properties of the integrands they can be expressed in terms of two independent integrals (cf Appendix A for more details):

$$\tilde{G}_{\mu\nu}^{(6,10)}(q, T) = -\frac{4}{9F^2} q_\mu q_\nu I(q, T) + \frac{9}{F^2} I_{\mu\nu}(q, T), \quad (3.25)$$

$$\begin{aligned} \tilde{G}_{\mu\nu}^{(6,11)}(q, T) = & \frac{\tilde{\Delta}(q)}{F^2} \left( \frac{8}{9} q_\mu q_\nu q^2 I(q, T) - 4q_\mu q^\rho I_{\nu\rho}(q, T) \right. \\ & \left. - 4q_\nu q^\rho I_{\mu\rho}(q, T) + 4q_\mu q_\nu \Delta_\beta^2(0) \right), \end{aligned} \quad (3.26)$$

$$\begin{aligned} \tilde{G}_{\mu\nu}^{(6,12)}(q, T) = & -q_\mu q_\nu \frac{\tilde{\Delta}^2(q)}{18F^2} \left\{ (5M^4 - 8q^4) I(q, T) \right. \\ & \left. + 72q^\rho q^\sigma I_{\rho\sigma}(q, T) - 12(M^2 - 3q^2) \Delta_\beta^2(0) \right\}. \end{aligned} \quad (3.27)$$

The functions  $I(q, T)$  and  $I_{\mu\nu}(q, T)$  are defined as:

$$I(q, T) = i \int \frac{d^d k_1 d^d k_2}{(2\pi)^{2d}} \tilde{\Delta}_\beta(k_1) \tilde{\Delta}_\beta(k_2) \tilde{\Delta}_\beta(q - k_1 - k_2), \quad (3.28)$$

$$I_{\mu\nu}(q, T) = i \int \frac{d^d k_1 d^d k_2}{(2\pi)^{2d}} \tilde{\Delta}_\beta(k_1) \tilde{\Delta}_\beta(k_2) \tilde{\Delta}_\beta(q - k_1 - k_2) k_{1\mu} k_{1\nu}. \quad (3.29)$$

These integrals have to be regularized because they are divergent in  $d = 4$ . Their finite parts are determined by the four functions  $\mathcal{N}_M(T)$ ,  $N_{\mu\nu}(M, T)$ ,  $\bar{I}(q, T)$  and  $\bar{I}_{\mu\nu}(q, T)$ , given in Appendix A.

The end result for the various terms appearing in the representation (3.2) reads:

$$\begin{aligned} \Xi(q, T) = & \bar{q}^2 + M_\pi^2 + \frac{M_\pi^2}{2F_\pi^2} \mathcal{N}_{M_\pi}(T) \\ & + \frac{1}{F_\pi^4} \left[ M_\pi^4 \bar{L}_\Xi \mathcal{N}_{M_\pi}(T) + \frac{M_\pi^4}{4} \mathcal{N}_{M_\pi}(T) \partial_{M_\pi^2} \mathcal{N}_{M_\pi}(T) \right. \\ & \left. - \frac{11M_\pi^2}{8} \mathcal{N}_{M_\pi}^2(T) + \frac{M_\pi^4}{6} \bar{I}(q, T) - q^\mu q^\nu \bar{\kappa}_{\mu\nu}(q, T) \right] + O(p^8), \end{aligned} \quad (3.30)$$

$$\begin{aligned} \alpha^A(q, T) = & F_\pi^2 - 2\mathcal{N}_{M_\pi}(T) \\ & + \frac{1}{F_\pi^2} \left[ M_\pi^2 \bar{L}_A \mathcal{N}_{M_\pi}(T) - M_\pi^2 \mathcal{N}_{M_\pi}(T) \partial_{M_\pi^2} \mathcal{N}_{M_\pi}(T) + 2\mathcal{N}_{M_\pi}^2(T) \right] + O(p^8), \end{aligned} \quad (3.31)$$

$$\beta_\mu^A(q, T) = \frac{1}{F_\pi^2} q^\nu \bar{\kappa}_{\mu\nu}(q, T) + O(p^8), \quad (3.32)$$

$$\gamma_{\mu\nu}^A = O(p^{10}), \quad (3.33)$$

$$\begin{aligned} \rho_{\mu\nu}^A(q, T) &= R_{\mu\nu}^A(q) + g_{\mu\nu} \alpha^A(q, T) \\ &+ \frac{1}{F_\pi^2} \left[ \bar{\kappa}_{\mu\nu}(q, T) + (q_\mu q_\nu - g_{\mu\nu} q^2) \left( 2\bar{L}_{10} - \frac{1}{72\pi^2} \right) \right] + O(p^8). \end{aligned} \quad (3.34)$$

The function

$$\bar{\kappa}_{\mu\nu}(q, T) := \bar{L} N_{\mu\nu}(M_\pi, T) + 4\bar{I}_{\mu\nu}(q, T), \quad (3.35)$$

and different combinations of the renormalized low-energy coupling constants were introduced to lighten the expressions:

$$\begin{cases} \bar{L} &= 32\bar{L}_1 + 64\bar{L}_2 - \frac{7}{18\pi^2} \\ \bar{L}_\Xi &= -48\bar{L}_1 - 16\bar{L}_2 + 48\bar{L}_4 - 80\bar{L}_6 - 40\bar{L}_8 + \frac{55}{576\pi^2} \\ \bar{L}_A &= 48\bar{L}_1 + 16\bar{L}_2 - 24\bar{L}_4 - \frac{7}{144\pi^2}. \end{cases} \quad (3.36)$$

Expressed in terms of the coupling constants defined in [4], these are given by

$$\begin{cases} \bar{L} &= (\bar{l}_1 + 4\bar{l}_2 - \frac{14}{3})/12\pi^2 \\ \bar{L}_\Xi &= (-24\bar{l}_1 - 16\bar{l}_2 + 15\bar{l}_3 + 12\bar{l}_4 + \frac{55}{3})/192\pi^2 \\ \bar{L}_A &= (6\bar{l}_1 + 4\bar{l}_2 - 9\bar{l}_4 - \frac{7}{3})/48\pi^2. \end{cases} \quad (3.37)$$

Note that  $\alpha^A(q, T)$  does not depend on the momentum at this order.

An integral representation can be given for the different functions of temperature and momentum appearing in the previous expressions.  $\mathcal{N}_M(T)$  has already been introduced in (3.13). The other function related to the properties of the propagator at the origin is  $N_{\mu\nu}(M, T)$ . It is given in Appendix A together with the regular parts of the momentum dependent functions  $I(q, T)$  and  $I_{\mu\nu}(q, T)$  defined in (3.28,3.29). All these functions depend on the ratio  $M/T$  in a non-trivial way.

The expressions (3.30-3.34) contain all the contributions to the finite temperature axial two-point Green's function to  $O(p^6)$ . Both  $M$  and  $T$  count as quantities of  $O(p)$ . The dependence of the functions  $\Xi(q, T)$ ,  $\alpha^A(q, T)$  and  $\beta_\mu^A(q, T)$  on the external momentum begins at this order. There is an important qualitative change between the one-loop and the two-loop results: the way the functions involved depend on  $q_0$  and on  $\vec{q}$  are now different, reflecting the breaking of Lorentz symmetry by the heat bath. As it must be, the  $T \neq 0$  renormalization is the same as the one at zero temperature [4].

## 4 The pion decay constants and mass at finite $T$

From the two-point axial Green's function some interesting quantities can be derived: the pion decay constants and mass. In the  $T = 0$  case the self-energy is defined as the pole of  $\tilde{G}_{\mu\nu}(q, T = 0)$  in the  $q_0$  complex plane and the pion decay constant as its residue at the pole position.

The dispersion curve determines the position of the pole in the  $q_0$ -plane:

$$q_0 = \Omega(\vec{q}, T). \quad (4.1)$$

In our case a non-trivial momentum dependence occurs at  $O(p^6)$ . Therefore the pole position at the same order can be obtained by replacing  $q_0$  by  $\omega_q = \sqrt{\vec{q}^2 + M_\pi^2}$ , that is:

$$\Omega^2(\vec{q}, T) = \Xi(q_0, \vec{q}, T) \Big|_{q_0=\omega_q} + O(p^8). \quad (4.2)$$

A possible definition of the mass is  $M_\pi(T) := \text{Re } \Omega(\vec{q}, T) \Big|_{\vec{q}=0}$ , i.e. the real part of the pole. With the  $\bar{L}$ s defined in (3.36), the ChPT result reads:

$$\begin{aligned} M_\pi^2(T) = & M_\pi^2 \left\{ 1 + \frac{1}{2F_\pi^2} \mathcal{N}_{M_\pi}(T) \right. \\ & + \frac{1}{F_\pi^4} \left[ M_\pi^2 \left( \mathcal{N}_{M_\pi}(T) \bar{L}_\Xi + \frac{1}{4} \mathcal{N}_{M_\pi}(T) \partial_{M_\pi^2} \mathcal{N}_{M_\pi}(T) \right) \right. \\ & \quad \left. + \frac{M_\pi^2}{6} \text{Re}[\bar{I}(q, T)] - \frac{11}{8} \mathcal{N}_{M_\pi}^2(T) \right. \\ & \quad \left. \left. - \bar{L} N_{00}(M_\pi, T) - 4 \text{Re}[\bar{I}_{00}(q, T)] \right] \Big|_{q_0=M, \vec{q}=0} \right\} + O(p^8). \end{aligned} \quad (4.3)$$

This result agrees with [7], where a somewhat different representation is used. The imaginary part of the pole, which determines the damping rate of the pions, has been thoroughly studied in the same context: its mean approximately behaves like  $T^5/F_\pi^5$  above 100 MeV [7].

To extract the residue at  $O(p^6)$ ,  $\Xi(q, T)$  has to be expanded around the pole position:

$$\Xi(q_0, \vec{q}, T) = \Omega^2(\vec{q}, T) + (q_0 - \omega_q) \frac{\partial \Xi(q, T)}{\partial q_0} \Big|_{q_0=\omega_q} + \dots \quad (4.4)$$

The thermal equilibrium state is invariant under spatial rotations, it implies that

$$\bar{\kappa}_{0i}(q, T) = q_i \bar{\kappa}(q, T), \quad (4.5)$$

thus  $\beta_\mu^A(q, T)$  can be rewritten as:

$$\beta_0^A(q, T) = q_0 \beta_t^A(q, T) \quad \text{and} \quad \beta_i^A(q, T) = q_i \beta_s^A(q, T). \quad (4.6)$$

The axial two-point function then takes the form

$$\tilde{G}_{\mu\nu}(q, T) = \Phi_{\mu\nu}^A(q, T) - \frac{f_\mu(q, T) f_\nu(q, T)}{q_0^2 - \Omega^2(\vec{q}, T)}, \quad (4.7)$$

where  $\Phi_{\mu\nu}^A(q, T)$  is a finite term and

$$\begin{cases} f_0(q, T) &= q_0 F_t(\vec{q}, T) \\ f_i(q, T) &= q_i F_s(\vec{q}, T). \end{cases} \quad (4.8)$$

The "temporal" residue at the pole position is given by

$$F_t^2(\vec{q}, T) = \left( \alpha^A(q, T) + 2\beta_t^A(q, T) \right) \left( 1 + \frac{1}{2\omega_q} \frac{\partial \Xi(q, T)}{\partial q_0} \right) \Big|_{q_0=\omega_q} + O(p^8). \quad (4.9)$$

The difference between  $\beta_t(q, T)$  and  $\beta_s(q, T)$  makes the difference in  $F_t(\vec{q}, T)$  and  $F_s(\vec{q}, T)$ .

The pion decay constants can naturally be defined as  $F_\pi^{s,t}(T) := F_{s,t}(\vec{q}, T) \Big|_{\vec{q}=0}$ . The ChPT computation gives

$$\begin{aligned} \left( F_\pi^t(T) \right)^2 &= F_\pi^2 \left\{ 1 - \frac{2}{F_\pi^2} \mathcal{N}_{M_\pi}(T) \right. \\ &\quad + \frac{1}{F_\pi^4} \left[ M_\pi^2 \left( \mathcal{N}_{M_\pi}(T) \bar{L}_A - \mathcal{N}_{M_\pi}(T) \partial_{M_\pi^2} \mathcal{N}_{M_\pi}(T) \right) \right. \\ &\quad \left. + \frac{M_\pi^3}{12} \frac{\partial}{\partial q_0} \bar{I}(q, T) + 2\mathcal{N}_{M_\pi}^2(T) + \bar{L} N_{00}(M_\pi, T) \right. \\ &\quad \left. \left. + 4\bar{I}_{00}(q, T) - 2M_\pi \frac{\partial}{\partial q_0} \bar{I}_{00}(q, T) \right] \Big|_{q_0=M, \vec{q}=0} \right\} + O(p^8) \end{aligned} \quad (4.10)$$

and the difference between the two pion decay constants is

$$\begin{aligned} \frac{F_\pi^t(T) - F_\pi^s(T)}{F_\pi} &= \frac{1}{F_\pi^4} \left[ \frac{1}{3} \bar{L} \left( 4N_{00}(M_\pi, T) - M_\pi^2 \mathcal{N}_{M_\pi}(T) \right) + \frac{4}{3} \mathcal{N}_M^2(T) \right. \\ &\quad \left. - \frac{4}{3} M_\pi^2 \bar{I}(q, T) + \frac{16}{3} \bar{I}_{00}(q, T) - M_\pi \bar{\kappa}(q, T) \right] \Big|_{q_0=M, \vec{q}=0} + O(p^8). \end{aligned} \quad (4.11)$$

The various functions of temperature involved in the expressions above are given in Appendix A.

The  $T$ -dependence and the evolution along the perturbation expansion of the mass and the "temporal" pion decay constant are displayed in Fig.3-4 in the case of the physical pion mass and pion decay constant:  $M_\pi \simeq 140$  MeV and  $F_\pi \simeq 93$  MeV. For both  $M_\pi(T)$  and  $F_\pi^t(T)$  the third order corrections have the opposite sign as those of the second order. At one loop, the mass is enhanced by the effects of the temperature, but the two-loop corrections bring it down (Fig.3). This may be a reflection of the fact that at  $T = 0$ , the first correction is negative for  $M$  (3.16). Exactly the opposite happens to the pion decay constant (Fig.4 and (3.16)). The difference between the "temporal" and "spatial" pion decay constants is always positive (cf Fig. 7 in the next Section).

## 5 Massless quarks

In our problem, the small  $M_\pi$  and fixed  $T$  case is equivalent to the limit  $T \gg M_\pi$ : only the ratio  $M_\pi/T$  is relevant. In the chiral limit, that is when the quark masses tends to zero,  $M_\pi$  tends to zero. The expressions of the pion decay constants and mass are much more readable ( $F \simeq 88$  MeV is the pion decay constant in the chiral limit [6]):

$$\left. \frac{M_\pi^2(T)}{M_\pi^2} \right|_{\hat{m}=0} = 1 + \frac{T^2}{24F^2} + \frac{T^4}{36F^4} \left[ \frac{19}{480} + K + \ln \frac{T}{\mu} - \frac{192\pi^2}{5} (L_1^r(\mu) + 2L_2^r(\mu)) \right] + O(T^6), \quad (5.1)$$

$$\left. \frac{\text{Re}(F_\pi^t(T))^2}{F_\pi^2} \right|_{\hat{m}=0} = 1 - \frac{T^2}{6F^2} + \frac{T^4}{36F^4} \left[ \frac{7}{60} - K - \ln \frac{T}{\mu} + \frac{192\pi^2}{5} (L_1^r(\mu) + 2L_2^r(\mu)) \right] + O(T^6), \quad (5.2)$$

$$\left. \frac{\text{Re}(F_\pi^t(T) - F_\pi^s(T))}{F_\pi} \right|_{\hat{m}=0} = \frac{T^4}{27F^4} \left[ -\frac{2}{15} - K - \ln \frac{T}{\mu} + \frac{192\pi^2}{5} (L_1^r(\mu) + 2L_2^r(\mu)) \right] + O(T^6). \quad (5.3)$$

Where the number

$$K = \ln 2 + \frac{1}{2}\Gamma'(1) + \frac{45}{\pi^4}\zeta'(4) - 1.05 \simeq -0.68 \quad (5.4)$$

contains the Euler gamma and Riemann zeta functions and a contribution from the integrals that had to be numerically evaluated.  $\mu$  is the regularization scale used in (3.12) and  $L_i^r(\mu) = \bar{L}_i + \gamma_i \ln \frac{\mu}{M}/(4\pi)^2$  are the scale-dependent renormalized effective coupling constants. The scale dependence and the logarithmic divergences of the individual terms appearing in (5.1-5.3) cancel, as they have to.

Our expressions for the pion mass and decay constants can always be written in the form

$$\left. \frac{M_\pi^2(T)}{M_\pi^2} \right|_{\hat{m}=0} = 1 + \frac{T^2}{24 F^2} - \frac{T^4}{36 F^4} \ln \frac{\Lambda_M}{T} + O(T^6), \quad (5.5)$$

$$\left. \frac{\text{Re}(F_\pi^t(T))^2}{F_\pi^2} \right|_{\hat{m}=0} = 1 - \frac{T^2}{6 F^2} + \frac{T^4}{36 F^4} \ln \frac{\Lambda_t}{T} + O(T^6), \quad (5.6)$$

$$\left. \frac{\text{Re}(F_\pi^t(T) - F_\pi^s(T))}{F_\pi} \right|_{\hat{m}=0} = \frac{T^4}{27 F^4} \ln \frac{\Lambda_\Delta}{T} + O(T^6). \quad (5.7)$$

Where  $\Lambda_{M,t,\Delta}$  are various scales which sizes are determined by the numbers and the values of the coupling constants appearing in (5.1-5.3). We take the recent two-loop evaluation [15] as reference:  $\bar{l}_1 = -1.7$  and  $\bar{l}_2 = 5.4$ , i.e.  $32\pi^2(\bar{L}_1 + 2\bar{L}_2) \simeq 1.66$ . The scale we find are rather big compared to the ones usually involved in ChPT [6]:

$$\Lambda_M \simeq 1.9 \text{ GeV} \quad (5.8)$$

$$\Lambda_t \simeq 2.3 \text{ GeV} \quad (5.9)$$

$$\Lambda_\Delta \simeq 1.8 \text{ GeV}. \quad (5.10)$$

In the range allowed for the temperature,  $\ln \Lambda_{M,t,\Delta}/T$  is positive. As already seen in the physical pion mass case, the third order corrections have the opposite signs to the second ones in  $M_\pi(T)$  and  $F_\pi^t(T)$ , whereas the latter is bigger than  $F_\pi^s(T)$ . This is shown in the Fig.5-7 both in the chiral limit and in the physical case.

To see what becomes the GOR relation at order  $T^4$ , we need the quark condensate to  $O(p^6)$ . It has been computed to  $O(p^8)$  in [6]. In the general case it reads:

$$\begin{aligned} \hat{m}\langle\bar{q}q\rangle_T &= \hat{m}\langle 0|\bar{q}q|0\rangle + \frac{3}{2}M_\pi^2\mathcal{N}_{M_\pi}(T) \\ &+ \frac{M_\pi^2}{F_\pi^2} \left[ M_\pi^2\mathcal{N}_{M_\pi}(T) \left( -24\bar{L}_4 + 48\bar{L}_6 + 48\bar{L}_8 + \frac{3}{64\pi^2} \right) \right. \\ &\quad \left. + \frac{3M_\pi^2}{4}\mathcal{N}_{M_\pi}(T) \partial_{M_\pi^2}\mathcal{N}_{M_\pi}(T) + \frac{3}{8}\mathcal{N}_{M_\pi}^2(T) \right] + O(p^8), \end{aligned} \quad (5.11)$$

thus in the chiral limit

$$\langle \bar{q}q \rangle_T \Big|_{\hat{m}=0} = \langle 0 | \bar{q}q | 0 \rangle \left\{ 1 - \frac{T^2}{8F^2} - \frac{T^4}{384F^4} \right\} + O(T^6). \quad (5.12)$$

Which means that a modified GOR relation can be written down for massless quarks at finite temperature:

$$\lim_{\hat{m} \rightarrow 0} \frac{M_\pi^2(T) \operatorname{Re}[(F_\pi^t(T))^2]}{\hat{m} \langle \bar{q}q \rangle_T} = -1 + O(T^6) \quad (5.13)$$

This was already noticed in [9] and [16] and is a consequence of the Goldstone theorem at finite temperature as will be seen in the next Section.

As expected, the essential characteristics of the low temperature behaviour of the three quantities examined are already present when the quark masses are sent to zero. Moreover, in this approximation a nice interpretation of the difference between the two pion decay constants and the imaginary parts of the residues of the two-point functions can be given. The next Section will come to that point.

Now, the symmetry groups occurring in the  $O(4)$  Linear Sigma Model (LSM) are the same as those of QCD with two massless flavours. Hence the effective field theories of these two systems are identical, only their effective coupling constants differs. This implies that the results obtained above are valid as they stand also for the  $O(4)$  model. In particular, the temperature expression of the pion mass contains a specific logarithmic contribution at order  $T^4$ . As it is absent in the LSM calculation described in [9, 17], their result is not complete at order  $T^4$ . The coupling constants  $L_1^r(\mu)$ ,  $L_2^r(\mu)$  can be evaluated for the LSM with [4]. The logarithmic contributions may be viewed as arising from a temperature dependent effective coupling constant of the LSM. Indeed, using the formula (34) in [9]

$$\frac{M_\pi^2(T)}{M_\pi^2} = 1 + \frac{T^2}{6F^2} - \frac{3\pi^2}{15} \frac{T^4}{F^2 m_\sigma^2}, \quad (5.14)$$

and replacing  $m_\sigma$  with  $m_\sigma(T)$  defined by

$$\frac{1}{m_\sigma^2(T)} := \frac{1}{m_\sigma^2} - \frac{5}{24\pi^2 F^2} \ln \frac{T}{\alpha m_\sigma}, \quad (5.15)$$

one recovers our result, provided that  $\alpha \simeq 0.68$ .

The same reasoning may be applied to the expressions found in [9] for both  $F_\pi^{s,t}(T)$ . Again the logarithms occurring at order  $T^4$  are missing. These expressions are compatible with ChPT if  $m_\sigma$  is replaced by  $m_\sigma(T)$  like in (5.14,5.15) but with  $\alpha \simeq 0.62$ . In the notation used above the difference between the two logarithmic scales arises from  $\Lambda_M \neq \Lambda_t$ . This difference also manifests itself in the temperature dependence



of the quark condensate at order  $T^4$ . If the formulae in [9] were correct, the temperature expression of the quark condensate would not contain a term of order  $T^4$ , in contradiction with the old calculation described in [6], where the result is given up to and including contributions of order  $T^6 \ln T$ .

## 6 Gell-Mann Oakes Renner relation at finite $T$

To see why the Gell-Mann Oakes Renner relation has to take the form (5.13) when  $T \neq 0$  and to compute the corrections in the quark mass is the main purpose of this Section. A possible way to do this is to go back where it originates at  $T = 0$ . It may be derived from two Ward Identities involving the quark condensate and both the axial and pseudoscalar two-point Green's functions. As already mentioned the difference between the  $T = 0$  and the  $T \neq 0$  cases is a change of manifold in the path integral formalism. Hence the derivation of Ward Identities from the generating functional of QCD at finite temperature go through the same steps as at  $T = 0$ . In the final equalities the vacuum expectation values of the involved operators are just replaced by their thermal average. These Ward Identities will be used both as a consistency check of the whole computation and as a source of the generalized relation. They will have byproducts which are going to clarify the meaning of our results.

To construct the finite temperature sisters of the Ward Identities which lead to the GOR relation at  $T = 0$ , one has to use the axial-vector current (3.1) and the pseudoscalar density

$$P^a(x) = \bar{q}(x) \frac{\tau^a}{2} i\gamma_5 q(x). \quad (6.1)$$

With the QCD Lagrangian, the following Ward Identities are obtained:

$$q^\mu \tilde{G}_{\mu\nu}(q, T) = 2\hat{m}\tilde{G}_\nu(q, T), \quad (6.2)$$

$$q^\mu \tilde{G}_\mu(q, T) = 2\hat{m}\tilde{G}(q, T) + \frac{1}{2} \langle \bar{q}q \rangle_T, \quad (6.3)$$

where  $G_{\mu\nu}(x, T)$  is the axial two-point Green's function defined in Section 3,  $G_\mu(x - y, T) \delta^{ab} := i\langle T A_\mu^a(x) P^b(y) \rangle_T$  and  $G(x - y, T) \delta^{ab} := i\langle T P^a(x) P^b(y) \rangle_T$ .

Note that at  $T = 0$ , both identities are fulfilled by ChPT. The first one implies that

$$2\hat{m}G_\pi = M_\pi^2 F_\pi, \quad (6.4)$$

and together with (6.3) in the chiral limit, one finds the GOR relation at zero temperature.

The new two-point functions are represented in the same way as the axial one (4.7):

$$\tilde{G}_\mu(q, T) = \Phi_{\mu\nu}^{AP}(q, T) - \frac{f_\mu(q, T) g(q, T)}{q_0^2 - \Omega^2(\vec{q}, T)}, \quad (6.5)$$

$$\tilde{G}(q, T) = \Phi^P(q, T) - \frac{g^2(q, T)}{q_0^2 - \Omega^2(\vec{q}, T)}. \quad (6.6)$$

$\Omega(\vec{q}, T)$  is defined as in (4.2) and the residue  $g(\vec{q}, T)$  similarly as the one of the axial two-point function (4.9). Again the strength of the coupling of the pseudoscalar density to the pion is defined to be  $G_\pi(T) := g(\vec{q}, T)|_{\vec{q}=0}$ , like in the axial case.

The first Ward Identity implies that

$$\Omega^2(\vec{q}, T) f_t(\vec{q}, T) - \vec{q}^2 f_s(\vec{q}, T) = 2\hat{m} g(q, T). \quad (6.7)$$

At  $\vec{q} = 0$ , it generates a relation very similar to (6.4):

$$2\hat{m}G_\pi(T) = \Omega^2(\vec{q}, T)|_{\vec{q}=0} F_\pi^t(T). \quad (6.8)$$

Then the second Ward Identity together with (6.7) implies that

$$-F_t(\vec{q}, T) g(\vec{q}, T) + q^\mu \Phi_\mu^{AP}(q, T) = 2\hat{m}\Phi^P(q, T) + \frac{1}{2}\langle\bar{q}q\rangle_T. \quad (6.9)$$

The quark condensate is independent of  $q$ . the previous equality can thus be evaluated in the chiral limit and at  $q = 0$  (or conversely). Together with (6.7) it gives a generalization of the GOR relation at finite temperature in a form very close to the one at  $T = 0$  (and to all orders in the perturbation theory):

$$\lim_{\hat{m} \rightarrow 0} \frac{\Omega(\vec{q}, T)|_{\vec{q}=0} (F_\pi^t(T))^2}{\hat{m}\langle\bar{q}q\rangle_T} = -1. \quad (6.10)$$

Because the quark condensate is a real quantity, the following relation must hold:

$$\lim_{\hat{m} \rightarrow 0} \frac{\text{Im}\left[\Omega(\vec{q}, T)|_{\vec{q}=0} (F_\pi^t(T))^2\right]}{\hat{m}} = 0. \quad (6.11)$$

Our result explicitly verifies this property at  $O(p^6)$ .

In order to compute the first corrections in the quark mass to the GOR relation at finite temperature, it is enough to compute the pseudoscalar two-point function. It requires the same building blocks as those of Section 3. Therefore only the end result will be given here. The graphs involved are the same as those appearing in Figure 2. The vertices are in general different and the diagrams (2.1, 4.1, 6.4, 6.7, 6.20) are zero, because  $\mathcal{L}^{(2)}$  is only linear in the pseudoscalar external field.

To present the result a representation similar as the one we used for the axial case in Section 3 is used:

$$\tilde{G}(q, T) = -\frac{\alpha^P(q, T)}{q_0^2 - \Xi(q, T)} + \rho^P(q, T) \quad (6.12)$$

The various functions appearing in the previous expression are found to be:

$$\begin{aligned} \alpha^P(q, T) &= G_\pi^2/B^2 - \mathcal{N}_{M_\pi}(T) \\ &+ \frac{1}{F_\pi^2} \left[ M_\pi^2 \bar{L}_P \mathcal{N}_{M_\pi}(T) - \frac{1}{2} M_\pi^2 \mathcal{N}_{M_\pi}(T) \partial_{M_\pi^2} \mathcal{N}_{M_\pi}(T) \right. \\ &\quad \left. - \frac{5}{2} \mathcal{N}_{M_\pi}^2(T) + \frac{M_\pi^2}{3} \bar{I}(q, T) \right] + O(p^8), \end{aligned} \quad (6.13)$$

$$\rho^P(q, T) = R^P(q) + \frac{1}{F_\pi^2} \left[ \bar{L}_\rho \mathcal{N}_{M_\pi}(T) - \frac{1}{6} \bar{I}(q, T) \right] + O(p^8), \quad (6.14)$$

where two new combinations of coupling constants have been used

$$\begin{cases} \bar{L}_P &= -48\bar{L}_1 - 16\bar{L}_2 + 104\bar{L}_4 - 224\bar{L}_6 - 112\bar{L}_8 + \frac{41}{288\pi^2} \\ \bar{L}_\rho &= 32\bar{L}_6 - 8\bar{L}_8 - \frac{3}{32\pi^2}. \end{cases} \quad (6.15)$$

The expression for  $\Xi(q, T)$  is the same as (3.30). This was a first test for the whole computation: the poles of the two Green's functions under consideration must be identical.

The corrections to the massless quark world can be computed. The first one that appears is

$$\frac{\Omega(\vec{q}, T) \Big|_{\vec{q}=0} (F_\pi^t(T))^2}{\hat{m} \langle \bar{q}q \rangle_T} = -1 + 2 \frac{M_\pi}{F_\pi^4} \frac{\partial}{\partial q_0} \bar{I}_{00}(q, T) \Big|_{q_0=M, \vec{q}=0} + O(M_\pi^2 \ln \frac{M_\pi}{T}, p^8), \quad (6.16)$$

the expansion of the last integral in terms of the pion mass is given in the Appendix B. We get:

$$\frac{\text{Re} \left[ \Omega(\vec{q}, T) \Big|_{\vec{q}=0} (F_\pi^t(T))^2 \right]}{\hat{m} \langle \bar{q}q \rangle_T} = -1 - \frac{M_\pi T^3}{F_\pi^4} \left( \frac{1}{24} - \frac{3}{4\pi^4} \zeta(3) \right) + O(M_\pi^2, M_\pi T^3 \ln \frac{M_\pi}{T}). \quad (6.17)$$

A small deviation linear in the pion mass is the first that appears. It is of the order of 6% at  $T = 100$  MeV and around 20% at 150 MeV. This is in contradiction to the QCD sum rule result obtained in [16], where the first correction is quadratic in  $M_\pi$ .

The Ward Identities (6.2,6.3) can be used as a consistency check of the whole calculation. The expressions for the quark condensate (5.11), the axial (3.2) and

the pseudoscalar (6.12) two-point Green's functions must fulfill the identities. It is here the case, irrespective of the specific forms of the different independent functions involved in them. This is also the case if one includes the imaginary parts of the finite terms that were ignored (see Section 3).

The relation (6.7) is very instructive in the chiral limit. It implies that

$$\Omega(\vec{q}, T) = \frac{\Theta_s^A(\vec{q}, T)}{\Theta_t^A(\vec{q}, T)} \vec{q}^2. \quad (6.18)$$

Thus the speed of the pions in the chiral limit is

$$v_\pi^2 \Big|_{\hat{m}=0} = 1 - \frac{\text{Re}\left(F_\pi^t(T) - F_\pi^s(T)\right)}{F_\pi} \Big|_{\hat{m}=0} + O(p^8). \quad (6.19)$$

It has to be smaller than the speed of light. Hence the difference between the real part of the two pion decay constants has to be positive (this remark was already made in [9]). Our result verifies this property. But looking at Fig. 7 or at (5.7), one sees that the square of the speed tends to zero at  $T \simeq 160$  MeV and even turns negative beyond that point. This is of course not allowed and it defines a natural limitation of the  $O(p^6)$  ChPT expansion.

Finally, because all the quantities involved in (6.18) are complex, this identity is in fact a system of two equalities containing six unknowns: the real and imaginary parts of the pole and of the two residues. Hence in the chiral limit,  $\text{Im}F_\pi^{s,t}(T)$  are completely determined by the other four quantities. Three of them are given in this article, whereas the imaginary part of the pole has been deeply studied in [7]. As a consequence, the physical content of the imaginary part of the residues encodes that of the other quantities involved, which physical interpretation is well known.

## 7 Summary and Conclusion

The dynamic of a pion travelling through a gas of pions at low temperature (up to circa 150 MeV) can be computed with the help of the ChPT Lagrangian. The knowledge of the effective mass is important to understand how this happens. The two different effective pion decay constants that appear because of the breaking of Lorentz symmetry by the equilibrium state are also quite meaningful. They were derived here to a  $T^4$  accuracy performing a two-loop calculation in ChPT. The temperature dependence of these interesting quantities is small. This is due to the size of the pion decay constant at  $T = 0$  which governs the ChPT expansion.

When the quark masses are sent to zero, contrary to the result obtained within the Linear Sigma Model in [9], we find a logarithmic dependence in the temperature

of the three mentioned observables at the two-loop order. The difference between the "temporal" and "spatial" pion decay constants is positive. This is related to the fact that the velocity of the pions in the gas is smaller than the speed of light. The Gell-Mann Oakes Renner relation is still satisfied, which is a reflection of the Goldstone theorem at finite  $T$ .

For realistic quark masses, the temperature dependence is quite obscure: it is contained in complicated integrals and some pictures are needed to see what happens. The behaviour of the pion decay constants and mass for the physical pion mass is not very different from the massless case.

The first corrections to the GOR relation are linear in the pion mass, they have a small magnitude. This does not agree with the result given in [16] using QCD sum rules.

Finally the presence of massive particles in the thermal equilibrium state deserves a comment. Their effects have been carefully analysed in [6]. The lightest ones that appear in our case are  $K(500)$  and  $\eta(550)$ . Their masses do not vanish in the chiral limit ( $m_{u,d} \rightarrow 0$ ). In our range of temperature, they behave like a dilute gas. They are of course exponentially suppressed, but their effects become more and more important when the temperature is increased. In the order parameter they generate a contribution of 0.5% at  $T = 100$  MeV with respect to that of the pions, whereas at  $T = 150$  MeV it becomes of the order of 10%. At  $T \simeq 160$  MeV, the mean distance between the massive states is approximately 1.6 fm and the number of massive particles per unit volume is the same as the numbers of pions. This gives a limitation to the ChPT approach. In the present calculation this limitation shows up at a similar temperature: the square of the velocity of propagation of the Goldstone bosons turns negative. Our results are meaningless beyond that point.

## Acknowledgements

It is a pleasure to thank H. Leutwyler for many useful discussions and a critical reading of the manuscript, U. Bürgi, J. Gasser and C. Hofmann for informative comments.

## A Properties of the $T$ -dependent integrals

A direct computation of the closed-eye, the guimbarde and the sunset graphs brings different complicated integrals. But taking into account the symmetry of the inte-

grands one can reduces them to two independent integral forms. A short notation is first introduced:

$$\langle f(q, k_1, k_2) \rangle := i \int \frac{d^d k_1 d^d k_2}{(2\pi)^{2d}} \tilde{\Delta}_\beta(k_1) \tilde{\Delta}_\beta(k_2) \tilde{\Delta}_\beta(q - k_1 - k_2) f(q, k_1, k_2). \quad (\text{A.1})$$

Because  $\langle f(q, k_1, k_2) \rangle = \langle f(q, k_2, k_1) \rangle = \langle f(q, q - k_1 - k_2, k_2) \rangle$  and that  $\langle k_1^2 \rangle = M^2 I(q, T) - \Delta_\beta^2(0)$ , the expressions for the closed-eye, the guimbarde and the sunset can be simplified into (3.22,3.23,3.24).

These two integrals  $I(q, T)$  and  $I_{\mu\nu}(q, T)$  diverge in  $d = 4$  dimensions. They have to be regularized. They contain three types of contributions. The  $T$ -independent terms are not of interest here. The parts involving one Bose distribution diverge for  $d = 4$  and the ones with a product of two statistical weights are finite for  $d = 4$ .

The first function of interest can be written as:

$$I(q, T) = \bar{I}(q, T) - 6\lambda \mathcal{N}_M(T) - \frac{3}{16\pi^2} \mathcal{N}_M(T), \quad (\text{A.2})$$

where  $\mathcal{N}_M(T)$ , already introduced in (3.13), is

$$\mathcal{N}_M(T) = \int \frac{d^4 k}{(2\pi)^3} \delta(k^2 - M^2) n_B(\omega_k), \quad (\text{A.3})$$

and  $\bar{I}(q, T)$  is a finite integral given by

$$\begin{aligned} \bar{I}(q, T) &= 3 \int \frac{d^4 k}{(2\pi)^3} \delta(k^2 - M^2) n_B(\omega_k) \bar{J}((q+k)^2) \\ &+ 3 \int \frac{d^4 k}{(2\pi)^3} \delta(k^2 - M^2) n_B(\omega_k) K(q+k, T) \\ &+ i \int \frac{d^4 k_1 d^4 k_2}{(2\pi)^6} \delta(k_1^2 - M^2) n_B(\omega_{k_1}) \delta(k_2^2 - M^2) n_B(\omega_{k_2}) \\ &\quad \delta((q - k_1 - k_2)^2 - M^2) n_B(\omega_{q-k_1-k_2}), \end{aligned} \quad (\text{A.4})$$

The second function we are interested in is

$$\begin{aligned} I_{\mu\nu}(q, T) &= \bar{I}_{\mu\nu}(q, T) \\ &+ \lambda \left( \mathcal{N}_M(T) \left[ g_{\mu\nu} \left( \frac{1}{3} q^2 - \frac{5}{3} M^2 \right) - \frac{4}{3} q_\mu q_\nu \right] - \frac{10}{3} N_{\mu\nu}(M, T) \right) \\ &+ \frac{1}{16\pi^2} \left( \mathcal{N}_M(T) \left[ \frac{1}{18} g_{\mu\nu} (q^2 + M^2) - \frac{5}{9} q_\mu q_\nu \right] - \frac{14}{9} N_{\mu\nu}(M, T) \right), \end{aligned} \quad (\text{A.5})$$

where  $N_{\mu\nu}(M, T)$  is

$$N_{\mu\nu}(M, T) = \int \frac{d^4 k}{(2\pi)^3} k_\mu k_\nu \delta(k^2 - M^2) n_B(\omega_k), \quad (\text{A.6})$$

and the finite integral  $\bar{I}_{\mu\nu}(q, T)$  is

$$\begin{aligned}
\bar{I}_{\mu\nu}(q, T) &= \int \frac{d^4k}{(2\pi)^3} \delta(k^2 - M^2) n_B(\omega_k) \bar{J}((q+k)^2) \\
&\quad \left\{ \frac{5}{3} k_\mu k_\nu + \frac{2}{3} q_\mu q_\nu + \frac{2}{3} (q_\mu k_\nu + q_\nu k_\mu) \right. \\
&\quad \left. + \left( \frac{M^2}{2} - \frac{q^2}{6} - \frac{qk}{3} \right) g_{\mu\nu} - \frac{2M^2}{3} \frac{(q_\mu + k_\mu)(q_\nu + k_\nu)}{(q+k)^2} \right\} \\
&+ \int \frac{d^4k}{(2\pi)^3} \delta(k^2 - M^2) n_B(\omega_k) \{ -2k_\mu K_\nu(q+k, T) \\
&\quad + K(q+k, T) [4k_\mu k_\nu + q_\mu q_\nu + 2(q_\mu k_\nu + q_\nu k_\mu)] \} \quad (\text{A.7}) \\
&+ i \int \frac{d^4k_1 d^4k_2}{(2\pi)^6} \delta(k_1^2 - M^2) n_B(\omega_{k_1}) \delta(k_2^2 - M^2) n_B(\omega_{k_2}) \\
&\quad \delta((q - k_1 - k_2)^2 - M^2) n_B(\omega_{q-k_1-k_2}) \\
&\quad \{ 4k_{1\mu} k_{1\nu} + q_\mu q_\nu - 2(q_\mu k_{1\nu} + q_\nu k_{1\mu}) + 2k_{1\mu} k_{2\nu} \}.
\end{aligned}$$

In (A.4,A.7), three one-loop functions have been introduced to get a simpler representation. The usual  $T = 0$  one

$$\bar{J}(q^2) = -\frac{1}{16\pi^2} \int_0^1 dx \ln(1 - q^2 x(1-x)/M^2), \quad (\text{A.8})$$

together with temperature dependent ones:

$$\begin{aligned}
K(q, T) &= i \int \frac{d^4k}{(2\pi)^3} \delta(k^2 - M^2) n_B(\omega_k) \tilde{\Delta}(q-k) \\
&= \frac{1}{16\pi^2 |\vec{q}|} \int_0^\infty dk \frac{k}{\omega_k} n_B(\omega_k) \ln \frac{(q^2 - 2k|\vec{q}|)^2 - 4\omega_k^2 q_0^2}{(q^2 + 2k|\vec{q}|)^2 - 4\omega_k^2 q_0^2} \\
&\quad + \frac{i}{8\pi |\vec{q}|} \int_0^\infty dk \frac{k}{\omega_k} n_B(\omega_k)
\end{aligned} \quad (\text{A.9})$$

and

$$\begin{aligned}
K_\mu(q, T) &= i \int \frac{d^4k}{(2\pi)^3} \delta(k^2 - M^2) n_B(\omega_k) \tilde{\Delta}(q-k) k_\mu \\
&= \frac{1}{\vec{q}^2} \left( n_\mu \left[ \frac{q_0}{2} \mathcal{N}_M(T) + \frac{q_0 q^2}{2} K(q, T) - q^2 K_0(q, T) \right] \right. \\
&\quad \left. - q_\mu \left[ \frac{1}{2} \mathcal{N}_M(T) + \frac{q^2}{2} K(q, T) - q_0 K_0(q, T) \right] \right),
\end{aligned} \quad (\text{A.10})$$

where  $n = (1, 0, 0, 0)$ . An integral representation for  $K_0(q, T)$  can be given:

$$K_0(q, T) = \frac{1}{16\pi^2 |\vec{q}|} \int_0^\infty dk k n_B(\omega_k) \ln \frac{q^4 - 4(\omega_k q_0 - k|\vec{q}|)^2}{q^4 - 4(\omega_k q_0 + k|\vec{q}|)^2} \quad (\text{A.11})$$

Note that because of the symmetry of the problem under spatial rotations:

$$N_{ik}(M, T) = \frac{1}{3} \delta_{ik} \left( N_{00}(M, T) - M^2 \mathcal{N}_M(T) \right), \quad (\text{A.12})$$

and

$$\bar{I}_{0i}(q, T) = q_i \bar{\kappa}(q, T)/4 \quad (\text{A.13})$$

$$\bar{I}_{ik}(q, T) = \delta_{ik} \bar{I}_1(q, T) + q_i q_k \bar{I}_2(q, T). \quad (\text{A.14})$$

The examined observables are defined on-shell at  $\vec{q} = 0$  and  $q_0 = M$ . In that special case, a simplified representation can be given. Note that because  $\omega_q \geq M$ , the different sums of  $T$ -independent one-loop functions appearing in the integrands can be rewritten as:

$$\begin{aligned} \bar{J}(2M^2 + 2M\omega_k) + \bar{J}(2M^2 - 2M\omega_k) &= \frac{1}{8\pi^2} \left( 2 + \frac{\omega_k}{|\vec{k}|} \ln \sigma(k) \right), \\ \bar{J}(2M^2 + 2M\omega_k) - \bar{J}(2M^2 - 2M\omega_k) &= \frac{1}{8\pi^2} \left( 2 + \frac{M}{|\vec{k}|} \ln \sigma(k) \right), \end{aligned} \quad (\text{A.15})$$

where

$$\sigma(k) := \frac{\sqrt{\omega_k + M} - \sqrt{\omega_k - M}}{\sqrt{\omega_k + M} + \sqrt{\omega_k - M}}. \quad (\text{A.16})$$

The following representations can be obtained:

$$\begin{aligned} \text{Re}[\bar{I}(q, T)] \Big|_{q_0=M, \vec{q}=0} &= \frac{3}{32\pi^4} \int_0^\infty dk \frac{k^2}{\omega_k} n_B(\omega_k) \left( 2 + \frac{\omega_k}{k} \log \sigma(k) \right) \\ &+ \frac{1}{16\pi^4} \int_0^\infty dk \int_0^1 d\alpha \frac{\alpha k^5}{\omega_\alpha \omega_k} n_B(\omega) n_B(\omega_\alpha) \ln \frac{1+\alpha}{1-\alpha} \end{aligned} \quad (\text{A.17})$$

$$\begin{aligned} \text{Re}[\bar{I}_{00}(q, T)] \Big|_{q_0=M, \vec{q}=0} &= \frac{1}{96\pi^4} \int_0^\infty dk \frac{k^2}{\omega_k} n_B(\omega_k) \left\{ (5k^2 + 7M^2) \right. \\ &\quad \left. \left( 2 + \frac{\omega_k}{k} \log \sigma(k) \right) + 2\omega_k M \left( 2 - \frac{M}{k} \log \sigma(k) \right) \right\} \\ &+ \frac{1}{16\pi^4} \int_0^\infty dk \int_0^1 d\alpha \alpha k^3 n_B(\omega_k) n_B(\omega_\alpha) \ln \tau(\alpha, k). \end{aligned} \quad (\text{A.18})$$

The expressions given above involve some new functions:

$$\omega_\alpha := \sqrt{\alpha^2 k^2 + M^2}, \quad (\text{A.19})$$



$$\tau(\alpha, k) := \frac{2k^2\alpha^2 + M^2(1 + \alpha^2) - 2\alpha\omega_k\omega_\alpha}{2k^2\alpha^2 + M^2(1 + \alpha^2) + 2\alpha\omega_k\omega_\alpha}. \quad (\text{A.20})$$

In general these integrals cannot be algebraically evaluated, even if the mass is zero.

Finally  $\bar{I}_{ik}(q, T)\big|_{q_0=M, \vec{q}=0}$  can be expressed in term of other known functions because of (A.14):

$$\bar{I}_{ik}(q, T)\big|_{q_0=M, \vec{q}=0} = \frac{1}{3} \delta_{ik} \left( \bar{I}_{00}(q, T) - M^2 \bar{I}(q, T) + \mathcal{N}_M^2(T) \right)\big|_{q_0=M, \vec{q}=0} \quad (\text{A.21})$$

## B Some functions in the chiral limit

As already mentionned all our integrals are in fact functions of  $M/T$ . It is however not so easy to evaluate the desired ones in the chiral limit. Some clever tricks can be found in [6]. The value of the four functions (3.13,A.3,A.17,A.18) in the chiral limit  $M \ll T$  is:

$$\begin{aligned} \mathcal{N}_M(T)\big|_{\hat{m}=0} &= \frac{T^2}{2\pi^2} \int_0^\infty dt t n_B(tT) - \frac{M}{2\pi^2 T} \int_1^\infty dt \frac{1}{t \sqrt{t^2 - 1}} + O\left(\frac{M^2}{T^2} \ln \frac{M}{T}\right) \\ &= \frac{T^2}{12} - \frac{MT}{4\pi} + O\left(\frac{M^2}{T^2} \ln \frac{M}{T}\right), \end{aligned} \quad (\text{B.1})$$

$$\begin{aligned} N_{00}(M, T)\big|_{\hat{m}=0} &= \frac{T^4}{2\pi^2} \int_0^\infty dt t^3 n_B(tT) + O\left(\frac{M}{T}\right) \\ &= \frac{\pi^2 T^4}{30} + O\left(\frac{M^2}{T^2}\right), \end{aligned} \quad (\text{B.2})$$

$$\text{Re}[\bar{I}(q, T)]\big|_{q=0, \hat{m}=0} = \frac{T^2}{64\pi^2} \ln \frac{M}{T} + O\left(\left(\frac{M}{T}\right)^0\right), \quad (\text{B.3})$$

$$\begin{aligned} \text{Re}[\bar{I}_{00}(q, T)]\big|_{q=0, \hat{m}=0} &= \frac{1}{2} \ln \frac{M}{T} \left( \mathcal{N}_M(T)\big|_{\hat{m}=0} \right)^2 \\ &\quad + \frac{5}{48\pi^2} \left( \ln \frac{M}{2T} + 2 \right) N_{00}(M, T)\big|_{\hat{m}=0} \\ &\quad + \frac{T^4}{2} \ln \frac{M}{2T} \left( \mathcal{N}_M(T) \right)^2 \\ &\quad + \frac{T^4}{8\pi^4} \int_0^\infty dt \int_0^1 d\alpha \alpha t^3 n_B(tT) n_B(\alpha tT) \ln \frac{1 + \alpha^2}{\alpha^2 k^2} \end{aligned} \quad (\text{B.4})$$

$$= T^4 \left( \frac{1}{144} \ln \frac{M}{T} - \frac{1}{144} \ln 2 + \frac{1}{1728} - \frac{\Gamma'(1)}{288} - \frac{5\zeta'(4)}{16\pi^4} + 0.0073 \right) + O\left(\frac{M}{T}\right).$$

The numbers appearing in the previous expressions are due to numerically evaluated integrals that come directly from the representations shown in Appendix A.

$$\begin{aligned} \bar{\kappa}(q, T) \Big|_{q=0, \hat{m}=0} &= \frac{1}{6M} (\mathcal{N}_M(T)|_{\hat{m}=0})^2 - \frac{5}{144M\pi^2} N_{00}(M, T)|_{\hat{m}=0} \\ &= O\left(\left(\frac{M}{T}\right)^0\right). \end{aligned} \quad (\text{B.5})$$

$$\begin{aligned} \frac{\partial}{\partial q_0} \text{Re}[\bar{I}_{00}(q, T)] \Big|_{q=0, \hat{m}=0} &= \frac{1}{2M} (\mathcal{N}_M(T)|_{\hat{m}=0})^2 - \frac{5}{48M\pi^2} N_{00}(M, T)|_{\hat{m}=0} \\ &\quad + \frac{3T^3}{16\pi^4} \int_0^\infty dt t^2 n_B(tT) \\ &= T^3 \left( \frac{3}{8\pi^4} \zeta(3) - \frac{1}{48\pi} \right) + O\left(\frac{M}{T} \ln \frac{M}{T}\right), \end{aligned} \quad (\text{B.6})$$

The cancellation of the  $1/M$  terms in the last integral in the chiral limit is very important for the safe of the GOR relation at finite temperature and the  $T^3$  term is responsible of the  $M_\pi T^3$  corrections (6.16).

## References

- [1] A.V. Smilga, "PHYSICS OF THERMAL QCD", TPI-MINN-96-23, hep-ph/9612347 and references therein.
- [2] M. Gell-Mann, R.J. Oakes and B. Renner, Phys. Rev. **175**, 2195 (1968).
- [3] S. Weinberg, Physica **A96**, 327 (1979).
- [4] J. Gasser and H. Leutwyler, Ann. Phys. **158**, 142 (1984).
- [5] J. Gasser and H. Leutwyler, Nuc. Phys. **B250**, 465 (1985).
- [6] P. Gerber and H. Leutwyler, Nuc. Phys. **B321**, 387 (1989).
- [7] A. Schenk, Phys.Rev. D **47**, 5138 (1993).

- [8] J. Gasser and H. Leutwyler, Phys. Lett. B **184**, 83 (1987), and **188** (1987) 477.
- [9] R.D. Pisarski and M. Tytgat, Phys. Rev. D **54**, 2989 (1996).
- [10] H. Leutwyler, Phys. Rev. D **49**, 3033 (1994).
- [11] N.P. Landsman and Ch.G. van Weert, Phys. Rep. **145**, 141 (1987) and references therein;  
 A.J. Niemi and G.W. Semenoff, Ann. Phys. **152**, 105 (1984); Nuc. Phys. B **230**, 181 (1984);  
 T. Altherr, Int. J. Mod. Phys. A **8**, 5605 (1993).
- [12] U. Bürgi, Nuc. Phys. B **479**, 392 (1996).
- [13] H.W. Fearing and S. Scherer, Phys. Rev. D **53**, 210 (1996).
- [14] J. Bijnens, G. Colangelo, G. Ecker, J. Gasser and M.E. Sainio, Phys. Lett. B **374**, 210 (1996).
- [15] G. Wanders, "CHIRAL TWO LOOP PION-PION SCATTERING PARAMETERS FROM CROSSING SYMMETRIC CONSTRAINTS", hep-ph/9705323.
- [16] C.A. Dominguez, M.S. Fetea and M. Loewe, Phys. Lett. B **387**, 151 (1996).
- [17] H. Itoyama and A. H. Mueller, Nucl. Phys. B **218**, 349 (1984).

## Figure Captions

**Fig. 1:** The Keldysh path of integration in the complex  $t$  plane. The arrows indicate the time ordering on each part of the contour. Only  $C_1$  and  $C_2$  are relevant in the generating functional.

**Fig. 2:** The Feynman diagrams necessary to compute the axial two-point Green's function to two loops. The various vertices correspond to the part of the effective Lagrangian (2.2) involved: the "dot" for the  $\mathcal{L}^{(2)}$  vertices, the "4" (resp. "6") for those of  $\mathcal{L}^{(4)}$  (resp.  $\mathcal{L}^{(6)}$ ). The wiggled lines represent an external field, whereas the plain lines are the thermal propagators. The various parts of the RTF propagator and the crossed graphs are not explicitly given.

**Fig. 3:** The effective pion mass at non-zero temperature. The dashed-dotted curve represents the trivial result at the tree level, the dashed one the one-loop computation and the full one the two-loop approximation.

**Fig. 4:** The real part of the "temporal" pion decay constant at non-zero temperature. The dashed-dotted curve represents the trivial result at the tree level, the dashed one the one-loop computation and the full one the two-loop approximation.

**Fig. 5:** The  $T$ -dependent pion mass to two loops in the chiral limit (dashed curve) and in the physical case (full one).

**Fig. 6:** The real part of the "temporal" pion decay constant to two loops in the chiral limit (dashed curve) and in the physical case (full one).

**Fig. 7:** The difference between the real parts of the "temporal" and "spatial" pion decay constants to two loops in the chiral limit (dashed curve) and in the physical case (full one). In the chiral limit this quantity is related to the speed of the pions.

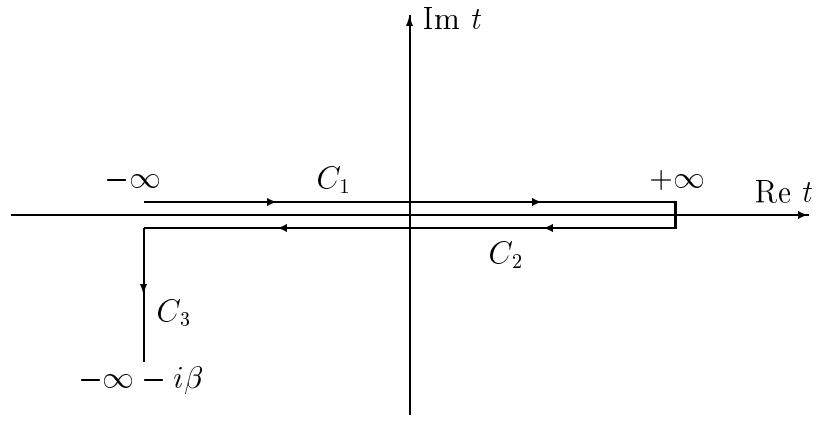


Fig. 1

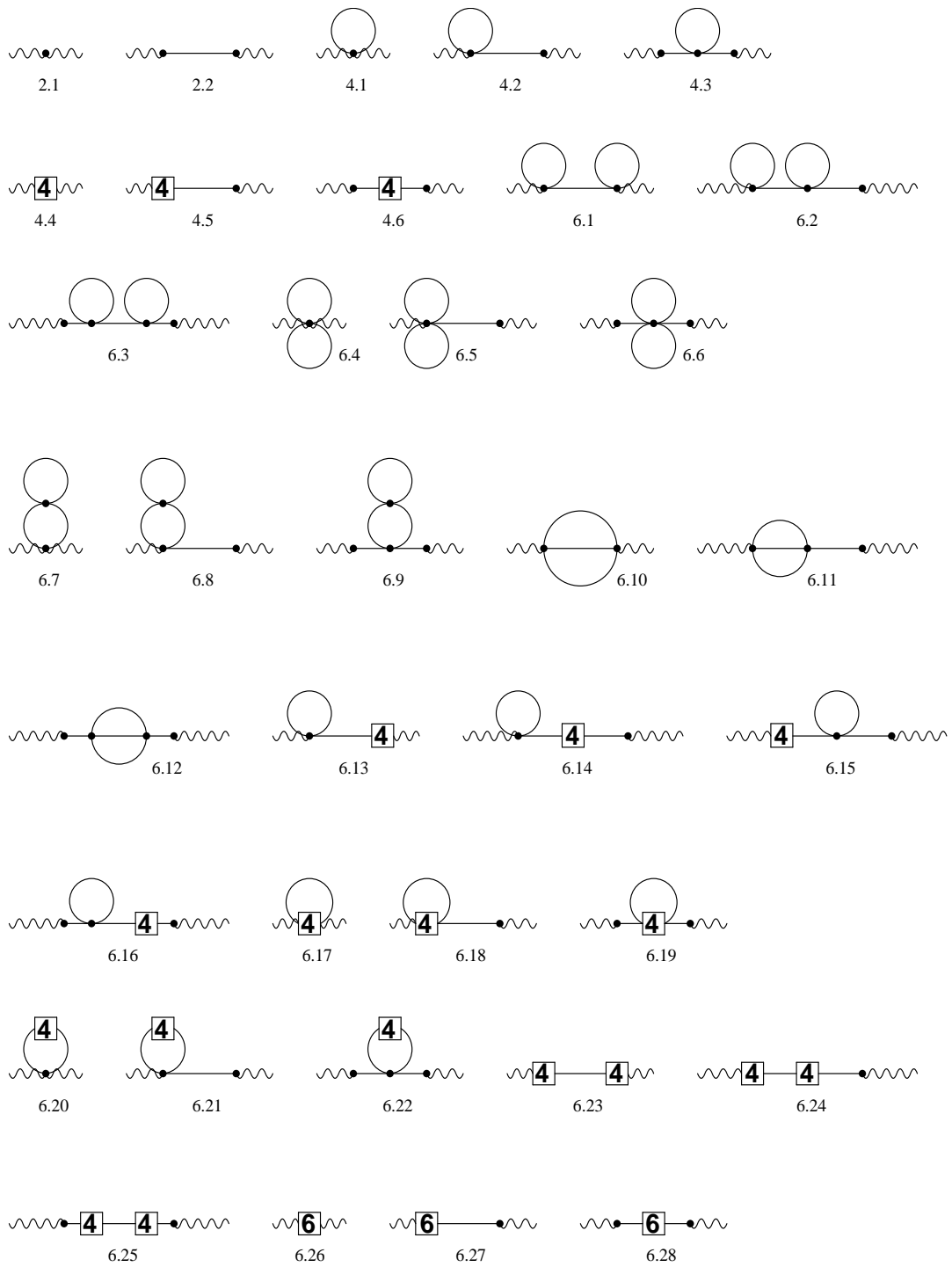


Fig. 2

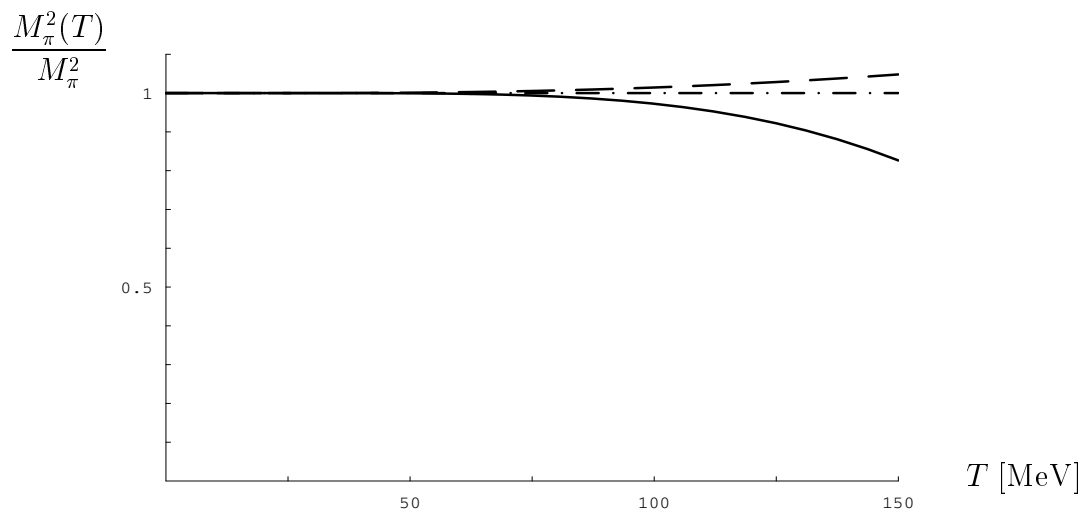


Fig. 3

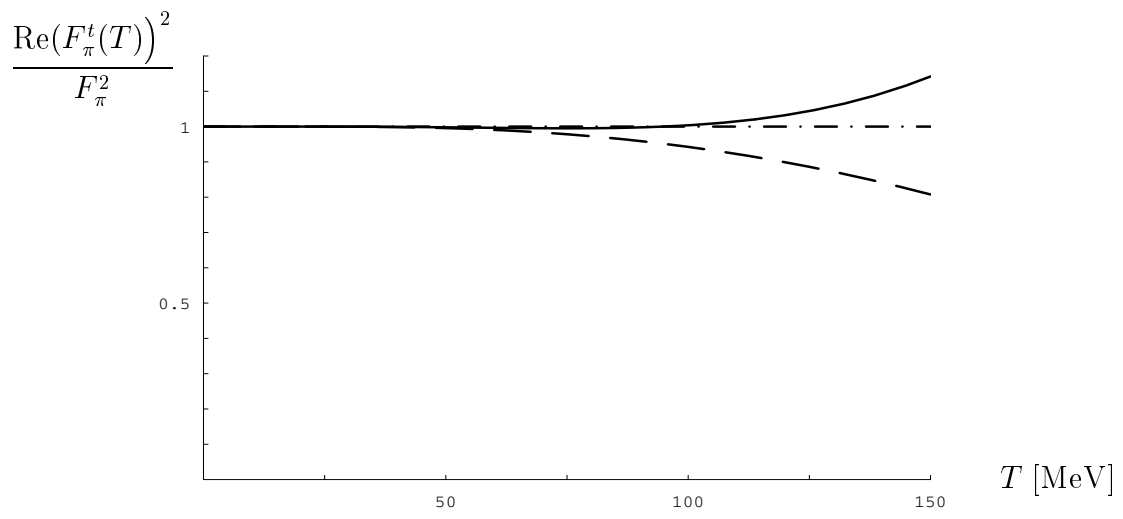


Fig. 4



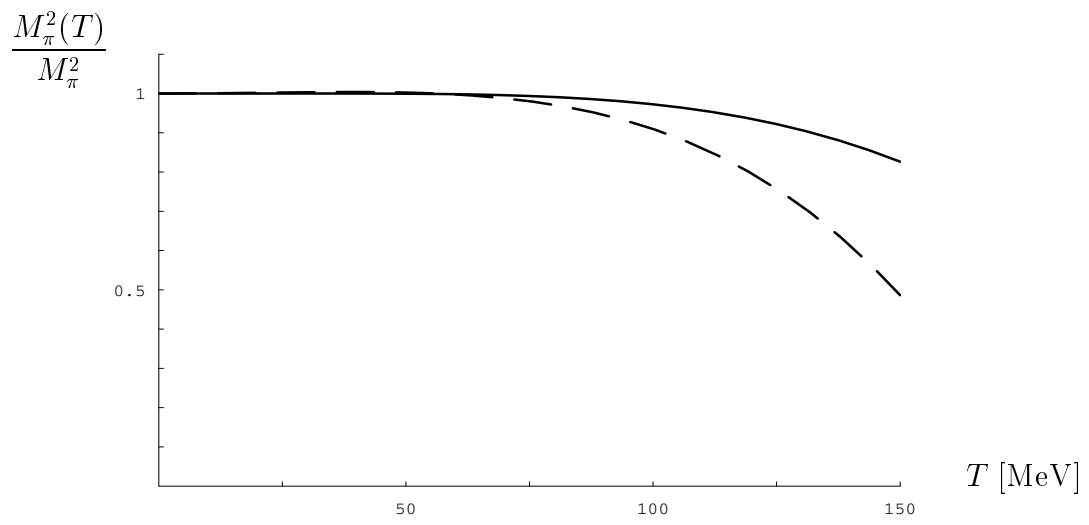


Fig. 5

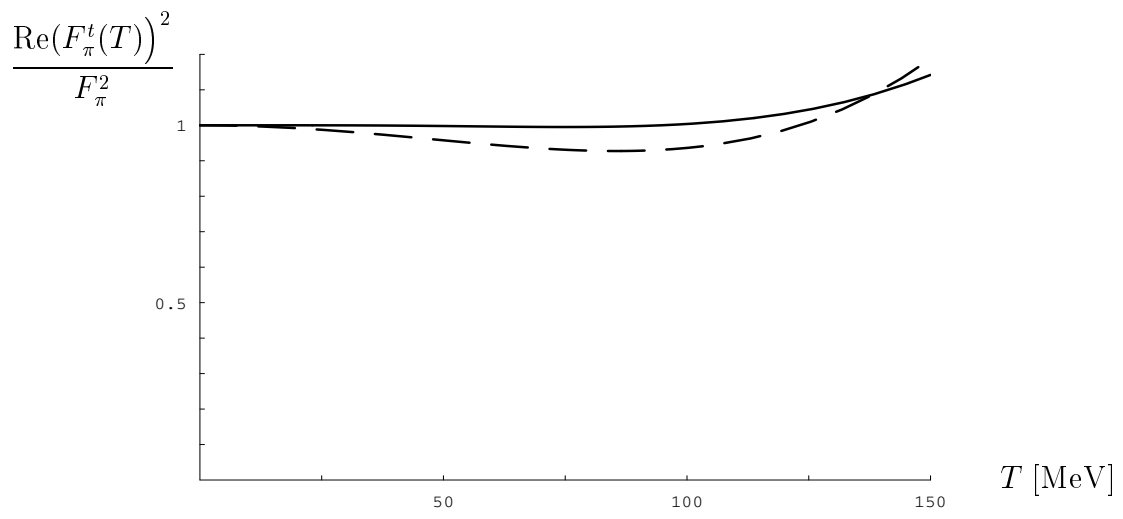


Fig. 6

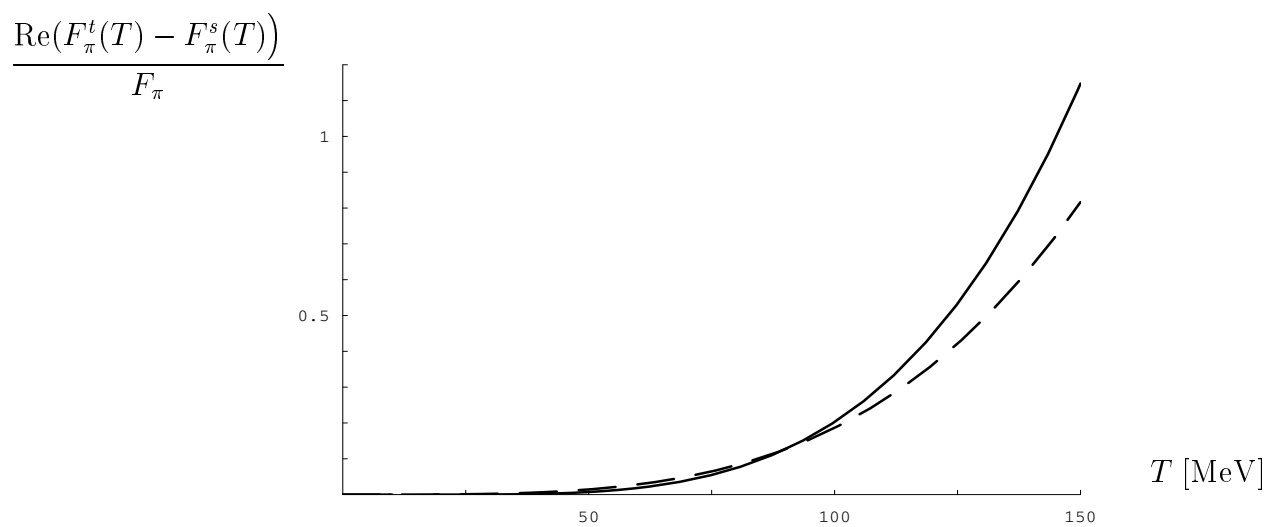


Fig. 7